Available online at www.sciencedirect.com
ScienceDirect
International Journal of Thermal Sciences 46 (2007) 467–478
International Journal of Thermal Sciences
www.elsevier.com/locate/ijts

Conjugate natural convection in a square enclosure with inclined thin fin of arbitrary length

Abdullatif Ben-Nakhi [a,*], Ali J. Chamkha [b]

[a] *Mechanical Power and Refrigeration Department, College of Technological Studies, PAAET, Kuwait*
[b] *Manufacturing Engineering Department, College of Technological Studies, PAAET, Kuwait*

Received 20 December 2005; received in revised form 3 July 2006; accepted 3 July 2006

Available online 22 August 2006

Abstract

This work is focused on the numerical study of steady, laminar, conjugate natural convection in a square enclosure with an inclined thin fin of arbitrary length. The inclined fin is attached to the left vertical thin side of the enclosure while the other three sides are considered to have finite and equal thicknesses of arbitrary thermal conductivities. The left wall of the enclosure to which the fin is attached is assumed heated while the external sides of the other three surfaces of the enclosure are cooled. The inclined thin fin is perfectly conductive and is positioned in the middle heated surface of the enclosure. Three different fin lengths equal to 20, 35 and 50 percent of the heated surface are considered. The problem is formulated in terms of the vorticity-stream function procedure. A numerical solution based on the finite-volume method is obtained. Representative results illustrating the effects of the thin fin inclination angle and length and the thermal conductivity of the thick surfaces on the streamlines and temperature contours within the enclosure are reported. In addition, results for the local and average Nusselt numbers are presented and discussed for various parametric conditions.

Keywords: Natural convection; Conjugate; Square enclosure; Thin fin; Inclined fin; Finite volume

1. Introduction

Natural convection in enclosures has attracted many researchers due to its wide range of applications, such as building thermal design, nuclear reactor design, solar energy collector, and others. The addition of a fin or array of fins to the enclosure surface(s) is a reliable method to increase the overall heat transfer rate between the heat dissipating surface(s) and the heat absorbing surface(s). Accordingly, the study of natural convection from finned surfaces has been the subject of many experimental and numerical investigations. These investigations are recently motivated by the advance in the electronics technology and the need for reliable and efficient cooling techniques. The increase in heat transfer rate due to the presence of a fin or array of fins depends greatly on the location, material and geometry of the fin(s). Starner and McManus [1] presented natural convection data for four different rectangular fin arrays attached to a horizontal, vertical and an inclined plate. A similar experimental study was carried out by Welling and Wooldridge [2]. They concluded that there exists an optimum fin height for every fin channel width. The flow pattern associated with free convection heat transfer from horizontal fin arrays has been also investigated by Harahap and McManus [3]. They showed that free convection heat transfer associated with a horizontally oriented fin array depends on the height of the fins.

Natural convection heat transfer in enclosures with various wall conditions have been extensively considered in the open literature. Owing the many possible practical applications, modification of heat transfer in cavities due to the presence of fin(s) attached to enclosure's wall(s) has received some consideration in recent years. Some of these applications can be found in solar collectors, nuclear reactors, heat exchangers and electronic equipment. Heat transfer rate through the enclosure can be controlled by means of fin's configuration. Oosthuizen and Paul [4] considered free convection heat transfer in a cavity

* Corresponding author. Current address: PO Box 3665, Salmiya, 22037 Kuwait. Tel.: +(965) 972 2700; Fax: +(965)561 8866.
E-mail address: abdnakhi@yahoo.com (A. Ben-Nakhi).

1290-0729/$ – see front matter
doi:10.1016/j.ijthermalsci.2006.07.008

Nomenclature

g	gravitational acceleration	$\mathrm{m\,s^{-2}}$
Gr	Grashof number, $= g\beta_T(T_\mathrm{h}-T_\mathrm{c})W^3/\nu^2$	
k	thermal conductivity	$\mathrm{W\,m^{-1}\,K^{-1}}$
l	fin length	m
L	dimensionless fin length, $= l/W$	
n	distance normal to s-axis	m
N	dimensionless n-coordinate, $= n/W$	
NNR	Nusselt number ratio at solid–fluid interface, $= \overline{Nu}_{\text{with fin}}/\overline{Nu}_{\text{no fin}}$	
Nu	local Nusselt number at solid–fluid interface	
$\overline{Nu}$	average Nusselt number at solid–fluid interface	
p	fluid pressure	Pa
Pr	Prandtl number, $= \nu/\alpha$	
Ra	Rayleigh number, $= g\beta_T(T_\mathrm{h}-T_\mathrm{c})W^3/(\alpha\nu)$	
s	coordinate adopted for distance along enclosure surfaces	m
S	dimensionless s-coordinate, $= s/W$	
T	temperature	K
u	x-component of velocity	$\mathrm{m\,s^{-1}}$
U	dimensionless X-component of velocity, $= uW/\alpha$	
v	y-component of velocity	$\mathrm{m\,s^{-1}}$
V	dimensionless Y-component of velocity, $= vW/\alpha$	
w	thickness of the cooled walls	m
W	horizontal/vertical dimension of the enclosure	m
x	horizontal distance	m
X	dimensionless horizontal distance, $= x/W$	
y	vertical distance	m
Y	dimensionless vertical distance, $= y/W$	
Z	dimensionless heated surfaces length, $= 1+2L$	

Greek symbols

ε	thin fin inclination angle	°
α	thermal diffusivity	$\mathrm{m^2\,s^{-1}}$
β_T	thermal expansion coefficient	$1\,\mathrm{K^{-1}}$
κ	solid-to-fluid thermal conductivity ratio, $= k_\mathrm{s}/k_\mathrm{f}$	
ν	kinematic viscosity	$\mathrm{m^2\,s^{-1}}$
θ	dimensionless temperature, $= (T-T_\mathrm{c})/(T_\mathrm{h}-T_\mathrm{c})$	
ρ	density	$\mathrm{kg\,m^{-3}}$
Ω	vorticity	$1\,\mathrm{s^{-1}}$
ω	dimensionless thickness of the thick walls, $= w/W$	
Ψ	stream function	$\mathrm{m^2\,s^{-1}}$
ψ	dimensionless stream function, $= \Psi/\alpha$	
$\Delta\psi_\mathrm{ext}$	change of extreme dimensionless stream function, $= \psi_\mathrm{max}-\psi_\mathrm{min}$	
ζ	dimensionless vorticity $= \Omega W^2/\alpha$	
∇^2	Laplacian operator	

Subscripts

c	cold surfaces
f	fluid
h	heated surfaces
s	solid

with aspect ratios between 3 and 7 with a horizontal plate fitted on the center of the vertical cold wall. Shakerin et al. [5] considered natural convection in an enclosure with discrete roughness elements on a vertical heated wall. Frederick [6] reported a parametric study of natural convection in an air-filled, differentially heated, inclined square cavity, with a fin attached perpendicularly to its cold wall at Rayleigh numbers of 10^3–10^5 and partition relative lengths of 0.25 and 0.5. It was reported that the fin causes convection suppression, and heat transfer reductions of up to 47% relative to the undivided cavity at the same Rayleigh number. Frederick and Valencia [7] considered heat transfer in a square cavity with a conducting partition at the center of its hot wall. They studied the impact of partition length and conductivity on heat transfer rate. Nag et al. [8] considered natural convection in a differentially heated square cavity with a horizontal partition plate on the hot wall. They analyzed the thermal effect of partition's length and location for Rayleigh number range from 10^3 to 10^6. Hasnaoui et al. [9] studied numerically a vertical rectangular differentially-heated enclosure with adiabatic fins attached to the heated wall. The enclosure aspect ratio was from 2 to 3, the dimensionless fin length from 0 to 0.75, and micro-cavity height from 0.30 to 0.67. Their study showed that the heat transfer through the cold wall was reduced compared to the case without fins and this reduction was enhanced with increasing fin length and decreasing Rayleigh number. Scozia and Frederick [10] considered natural convection heat transfer in a differentially-heated slender rectangular cavity of aspect ratio of 20 with multiple conducting fins attached on the active cold wall of the cavity. They concluded that as the inter-fin aspect ratio was varied from 20 to 0.25, the flow patterns evolved considerably and the average Nusselt number exhibited maximum and minimum values whose locations depended on the value of the Rayleigh number. Facas [11] studied natural convection in a slender cavity of aspect ratio of 15 with fins attached to both vertical differentially-heated walls. For small fin lengths, the flow was slightly blocked and a multicellular flow structure was observed. For longer fin lengths, the flow was blocked further and secondary recirculation cells were formed, in addition to the primary recirculation. As a result, higher heat transfer rates across the two sides of the cavity were observed. Lakhal et al. [12] considered natural convection in inclined rectangular enclosures of aspect ratios of 2.5 or higher with perfectly conducting fins attached on the heated wall. They have found that the flow regime at low Rayleigh number is one of pure conduction and the heat losses through the cold wall can be reduced considerably by using fins attached on the heated wall. Bilgen [13] studied natural convection in enclosures with partial partitions attached to the adiabatic horizontal surfaces. His study covered various geometrical parameters: enclosure aspect ratio = 0.3–0.4, number of partitions = 1 or 2, partitions dimensionless position = 0.5–0.6, partitions dimensionless height = 0.0–0.15, $Ra = 10^4$–10^{11}. The results showed

that the flow regime was laminar for Ra up to 10^8 thereafter turbulent. The heat transfer was reduced (a) when two partitions were used instead of one, (b) when the aspect ratio was made smaller, (c) when the position of partitions was farther away from the hot wall. Shi and Khodadadi [14] reported a detailed parametric study of flow and heat transfer in a lid-driven cavity due to the presence of a single thin fin. Three fins with lengths equal to 5, 10, and 15 percent of the side, positioned at 15 locations were examined for $Re = 500$, 1000, 2000, and $Pr = 1$. They concluded that the fin slows the flow near the anchoring wall and reduces the temperature gradients, thus degrading heat transfer capacity. Shi and Khodadadi [15] also studied steady laminar natural convection within a differentially heated square cavity due to the presence of a single highly conductive thin fin. The study covered three fin lengths, seven fin locations, and $Ra = 10^4$–10^7. They have stated that for high Rayleigh numbers the flow field is enhanced regardless of the fin's length and position indicating that the extra heating mechanism outweighs the fin's blockage effect. They also reported that better heat transfer performance can be achieved if the thin fin attached to the hot wall was closer to the insulated walls. Bilgen [16] considered natural convection in differentially heated square cavities with horizontal thin fin for Rayleigh number from 10^4 to 10^9. The cavity was formed by vertical isothermal walls and adiabatic horizontal walls. A thin fin was attached to the hot side. The parametric study covered fin's dimensionless length from 0.10 to 0.90, fin's dimensionless position from 0.10 to 0.90, and fin's relative conductivity from 1 to 60. Inclined thin fin was first considered by Ben-Nakhi and Chamkha [17] who studied the effects of a heated thin fin length and inclination angle on steady, laminar, two-dimensional natural convection fluid flow inside a differentially-heated square enclosure. The study covered fin inclination angles from 0° to 180°, and dimensionless fin lengths of 0.2, 0.35, and 0.5.

Many researchers have studied the impact of coupling wall conduction with natural convection in enclosures. The results of their works clearly indicate that the conjugate heat transfer parameter has a significant influence on the fluid flow and heat transfer characteristics in comparison with those reported for isothermal thin walls. Kim and Viskanta [18] studied the effects of wall conduction and radiation heat exchange among surfaces on laminar natural convection heat transfer in a differentially heated two-dimensional rectangular cavity with four thick walls. Their results indicate that natural convection heat transfer in the cavity is reduced by heat conduction in the walls. Kaminski and Prakash [19] analyzed steady laminar natural convection flow in a square enclosure with one vertical conducting wall. They concluded that for Grashof number greater than 10^5, the temperature distribution in the wall shows significant two-dimensional effects and the solid–fluid interface temperature is found to be quite non-uniform. Du and Bilgen [20] considered conjugate heat transfer in an enclosure which consists of a conducting vertical wall of finite thickness with a uniform heat input, an insulated vertical wall and two horizontal walls at a heat sink temperature. They reported that for low Ra, high solid–fluid conductivity ratio, and high dimensionless wall thickness at small and large enclosure aspect ratio, the heat transfer process is dominated by the heat conduction in the solid wall. For high Ra, low solid–fluid conductivity ratio, and low dimensionless wall thickness at moderate enclosure aspect ratio, strong interaction between conduction in the solid wall and convection in the fluid influences the heat transfer. Liaqat and Baytas [21] analyzed laminar natural convection flow in a square enclosure having thick conducting walls. Their conjugate analyses showed a significant change in the buoyant flow parameters as compared to conventional non-conjugate analyses.

The purpose of the present work is to study conjugate natural convection inside a square enclosure in the presence of a perfectly conductive inclined thin fin of arbitrary length attached at the center of the left heated thin vertical surface. The other three surfaces of the enclosure are assumed to have finite and equal thicknesses of conductive solid material and their external sides are cooled. The effects of fin length and inclination angle and the solid-to-fluid thermal conductivity ratio on the flow and heat transfer characteristics are studied.

2. Mathematical model

Consider steady laminar, two-dimensional, conjugate natural convection inside a square enclosure in the presence of a perfectly conductive inclined thin fin of arbitrary length attached at the center of the left heated vertical surface. As shown in Fig. 1, the left vertical surface of the enclosure is assumed to have a negligible thickness while the remaining three surfaces are of finite thicknesses of arbitrary thermal conductivity. The left vertical surface is uniformly heated and maintained at a temperature T_h whereas the external sides of the other three thick surfaces are uniformly cooled and maintained at a tem-

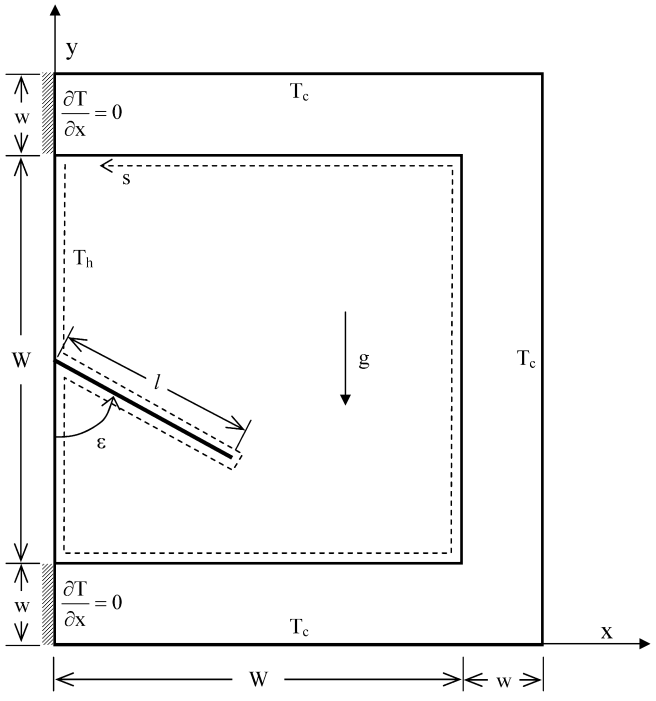

Fig. 1. Schematic diagram and coordinate system for a square enclosure with inclined fin at the center of the hot wall.

perature T_c. The fluid is assumed to be incompressible, viscous, and Newtonian having constant thermo-physical properties.

The governing equations for this problem are based on the balance laws of mass, linear momentum and energy. Taking into account the assumptions mentioned above, and applying the Boussinesq approximation for the body force terms in the momentum equations, the governing equations can be written in dimensionless vorticity-stream function formulation as:

$$\zeta = \frac{\partial V}{\partial X} - \frac{\partial U}{\partial Y} = -\nabla^2 \psi \tag{1}$$

$$U\frac{\partial \zeta}{\partial X} + V\frac{\partial \zeta}{\partial Y} = Pr\nabla^2 \zeta + Ra\,Pr\left(\frac{\partial \theta}{\partial X}\right) \tag{2}$$

$$U\frac{\partial \theta}{\partial X} + V\frac{\partial \theta}{\partial Y} = \nabla^2 \theta \tag{3}$$

For the solid region,

$$\nabla^2 \theta = 0 \tag{4}$$

The boundary conditions in dimensionless form become

At all walls and in the solid region $U = V = \psi = 0$. e5

$$X = 0,\ 0 \leqslant Y < \omega \quad \frac{\partial \theta}{\partial X} = 0 \tag{5a}$$

$$X = 0,\ \omega \leqslant Y \leqslant 1 + \omega \quad \zeta = -\left(\frac{\partial^2 \psi}{\partial X^2}\right), \quad \theta = 1.0 \tag{5b}$$

$$X = 0,\ 1 + \omega < Y \leqslant 1 + 2\omega \quad \frac{\partial \theta}{\partial X} = 0 \tag{5c}$$

$$X = 1,\ \omega \leqslant Y \leqslant 1 + \omega$$
$$\zeta = -\left(\frac{\partial^2 \psi}{\partial X^2}\right), \left(\frac{\partial \theta}{\partial X}\right)_{\text{fluid}} = \kappa\left(\frac{\partial \theta}{\partial X}\right)_{\text{solid}} \tag{5d}$$

$$X = 1 + \omega \quad \theta = 0.0 \tag{5e}$$

$$Y = 0 \quad \theta = 0.0 \tag{5f}$$

$$Y = \omega,\ 0 < X < 1$$
$$\zeta = -\left(\frac{\partial^2 \psi}{\partial Y^2}\right), \left(\frac{\partial \theta}{\partial Y}\right)_{\text{fluid}} = \kappa\left(\frac{\partial \theta}{\partial Y}\right)_{\text{solid}} \tag{5g}$$

$$Y = 1 + \omega,\ 0 < X < 1$$
$$\zeta = -\left(\frac{\partial^2 \psi}{\partial Y^2}\right), \left(\frac{\partial \theta}{\partial Y}\right)_{\text{fluid}} = \kappa\left(\frac{\partial \theta}{\partial Y}\right)_{\text{solid}} \tag{5h}$$

$$Y = 1 + 2\omega \quad \theta = 0.0 \tag{5i}$$

$$\text{On the fin} \quad \theta = 1.0 \tag{5j}$$

In writing Eqs. (1)–(5) the following dimensionless parameters and definitions are used:

$$X = \frac{x}{W}, \qquad Y = \frac{y}{W}$$

$$\zeta = \frac{\Omega W^2}{\alpha}, \qquad \psi = \frac{\Psi}{\alpha}$$

$$Pr = \nu/\alpha, \qquad \theta = \frac{(T - T_c)}{(T_h - T_c)}$$

$$Ra = \frac{g\beta_T (T_h - T_c) W^3}{\alpha \nu}$$

$$\Omega = -\left(\frac{\partial^2 \Psi}{\partial x^2} + \frac{\partial^2 \Psi}{\partial y^2}\right)$$

$$v = -\frac{\partial \Psi}{\partial x}, \qquad u = \frac{\partial \Psi}{\partial y} \tag{6}$$

The average Nusselt number of the heated surfaces (left vertical wall including both sides of thin fin) $\overline{Nu}_h$ and the average Nusselt number at the cold surfaces of the enclosure $\overline{Nu}_c$ are, respectively, given by:

$$\overline{Nu}_h = -\frac{1}{Z}\int_0^Z \left(\frac{\partial \theta}{\partial N}\right) dS, \quad \text{where } Z = 1 + 2L \tag{7}$$

$$\overline{Nu}_c = -\frac{1}{3}\int_{1+2L}^{4+2L} \left(\frac{\partial \theta}{\partial N}\right) dS \tag{8}$$

In order to monitor the qualitative effect of the presence of the thin fin on the average heat transfer rate, the Nusselt number ratio is introduced as:

$$NNR = \frac{\overline{Nu}_{\text{with fin}}}{\overline{Nu}_{\text{no fin}}} \tag{9}$$

3. Numerical algorithm

The governing equations (1)–(4) for steady, laminar, two-dimensional conjugate natural convection heat transfer in a square enclosure with inclined thin fin are solved by using the Gauss–Seidel point-by-point method as discussed by Patankar [22] along with under-relaxation factors for temperature, vorticity, and stream functions. The convective terms were approximated by the second-order upwind discretization scheme and the diffusive terms with the central differencing scheme. The convergence criterion employed was the standard relative error, which is based on the maximum norm given by

$$\Delta = \frac{\|\zeta^m - \zeta^{m-1}\|_\infty}{\|\zeta^m\|_\infty} + \frac{\|\theta^m - \theta^{m-1}\|_\infty}{\|\theta^m\|_\infty} \leqslant 10^{-6} \tag{10}$$

where the operator $\|\eta\|_\infty$ indicates the maximum absolute value of the variable over all the grid points in the computational domain and m and $m-1$ represent the current and previous iteration, respectively.

An unstructured grid of tri-angular mesh elements was employed in the current work. Numerical tests were performed to select the suitable mesh resolution. Extensive tests were carried out to ascertain grid convergence by deploying meshes of 11 892, 15 537, 19 621, and 25 324 nodes. The average Nusselt number at the heated surfaces $\overline{Nu}_h$ was monitored in the grid dependence test. Accordingly, the mesh of 19 621 nodes was used in the current work as the difference between $\overline{Nu}_h$ values for the finest two meshes is less than 1%. The mesh quality of the numerical model was further assessed by means of Aspect Ratio, EquiAngle Skew, and EquiSize Skew of each cell within the domain. The definitions and acceptable ranges for the employed mesh quality indices are described elsewhere [17]. With respect to the Aspect Ratio, 90% of the cells have $1.0 \leqslant Q_{AR} \leqslant 1.01$ and 99% of the cells have $1.0 \leqslant Q_{AR} \leqslant 1.08$. From EquiAngle Skew viewpoint, 90% of the cells have $0.0 \leqslant Q_{EAS} \leqslant 0.08$ and 99% of the cells have $0.0 \leqslant Q_{EAS} \leqslant 0.24$. Furthermore, 90%

Table 1
Comparison of the predicted average Nusselt number $\overline{Nu}$ on the solid/fluid interface of a differentially-heated enclosure without a fin with Refs. [19,21]

Gr	κ	Kaminski and Prakash [19]	Liaqat and Baytas [21]	Present work
10^3	1	0.87	0.88	0.87
	5	1.02		1.02
	10	1.04		1.04
	∞	1.06	1.07	1.06
10^5	1	2.08	2.08	2.08
	5	3.42		3.42
	10	3.72		3.72
	∞	4.08	4.12	4.07
10^6	1	2.87	2.84	2.86
	5	5.89		5.91
	10	6.81		6.84
	∞	7.99	8.07	8.09

of the cells have EquiSize Skew Q_{ESS} of $0.0 \leqslant Q_{\mathrm{ESS}} \leqslant 0.01$ and 99% of the cells have $0.0 \leqslant Q_{\mathrm{ESS}} \leqslant 0.1$.

In order to reduce round-off error, double precision computation was employed. The accuracy of numerical scheme is validated by comparing the average Nusselt number $\overline{Nu}$ for a differentially-heated square enclosure in the absence of the fin under various Grashof numbers with those reported by Kaminski and Prakash [19] and Liaqat and Baytas [21] as shown in Table 1. These comparisons show good agreement. In addition, the numerical scheme is validated by comparing against the results of various cases of the problem of Shi and Khodadadi [15] who considered a similar configuration with a non-inclined fin, thin walls, and adiabatic boundaries at the horizontal sides of the cavity. Good agreement with the results of Shi and Khodadadi [15] is observed as is evident from Fig. 2. Further validation is performed by comparing against the results of various cases with inclined fin presented previously by Ben-Nakhi and Chamkha [17] who considered a configuration that is similar to that of Shi and Khodadadi [15] but with an inclined fin. Excellent agreement was achieved for all cases considered, however, the results are not presented in this paper due to space limitations. It should be mentioned here that thermal conductivities of the vertical and horizontal thick walls were set to 10^{12} and 10^{-12} $\mathrm{W\,m^{-1}\,K^{-1}}$, respectively, during the validation process in order to mimic the thin walls situation with their appropriate boundary conditions. These favorable comparisons lend confidence in the numerical results to be presented in the next section.

4. Result and discussion

In this section, numerical results for the streamline and temperature contours for various values of the fin inclination angle ε, fin dimensionless length L, solid-to-fluid thermal conductivity ratio κ, and the Rayleigh number Ra will be reported. All results are computed for a Prandtl number $Pr = 0.707$ and a dimensionless solid wall thickness $\omega = 0.2$. In addition, the effects of κ and L on the change of the extreme dimensionless stream function $\Delta\psi_{\mathrm{ext}}$ will be shown and analyzed. Furthermore, representative results for the local, average and the Nusselt number ratio (Nu, $\overline{Nu}$, and NNR) for various conditions will be presented and discussed.

Fig. 3 presents steady-state contour plots for the streamline and temperature for various values of κ for a square enclosure without a fin ($\varepsilon = 0°$ or $\varepsilon = 180°$). It should be noted that small values of κ correspond to pronounced thick wall effect while large values of κ correspond to minimized thick wall effect and $\kappa = \infty$ correspond to the thin wall condition. The rise of the fluid due to buoyancy effects caused by heating of the left wall of the enclosure and the consequent falling of the fluid on the right and horizontal cold walls creates a clockwise-rotating vortex. It is observed that the strength or values of the streamlines increase as κ increases. In addition, the isotherms are stretched in the thick wall regions for small values of κ while they become more contained within the main enclosure as κ increases. In fact, the thick wall effects diminish completely as they should as $\kappa \to \infty$.

Fig. 4 illustrates the effect of increasing the solid-to-fluid thermal conductivity ratio κ from $\kappa = 1$ to $\kappa = \infty$ on the streamline and isotherms in the presence of a thin fin inclined at angle $\varepsilon = 105°$ and having a dimensionless length $L = 0.35$. In general, it is seen that the presence of the inclined fin at the center of the heated surface of the enclosure splits the main vortex in the enclosure creating a secondary vortex close to the upper horizontal surface which remains attached to the main vortex. As κ increases, $\Delta\psi_{\mathrm{ext}}$ increases and the secondary vortex tends to stretch closer to the upper left corner of the enclosure. By comparison with Fig. 3 for the case of no fin present, it can be seen that in the presence of the inclined fin, the rate of increase of $\Delta\psi_{\mathrm{ext}}$ as κ increases is slower than that of the no-fin case. This is expected since the presence of the fin presents an obstacle to the clockwise flow caused by the thermal buoyancy effect. In addition, the effect of κ on the isotherms is similar to that observed in the case of no fin. That is, strong thick wall thermal effects are predicted for small values of κ and these effects reduce as κ increases reaching the case of no effects as $\kappa \to \infty$.

Fig. 5 depicts the effects of increasing κ and ε on the values of $\Delta\psi_{\mathrm{ext}}$ for $L = 0.35$. In general, increasing κ decreases the temperature drop in the thick walls. Accordingly, the effective temperature difference driving the flow in the enclosure is increased resulting in increased buoyancy-induced flow represented by higher values of $\Delta\psi_{\mathrm{ext}}$. For all values of κ, as ε increases, $\Delta\psi_{\mathrm{ext}}$ increases reaching a maximum at $\varepsilon = 90°$ and then dips down to a relative minimum at $\varepsilon = 120°$ before it increases again as ε increases further. However, for $\kappa = 1$, $\Delta\psi_{\mathrm{ext}}$ decreases slowly from its maximum value at $\varepsilon = 90°$ as ε increases beyond 90°. On the other hand, the relation between L and $\Delta\psi_{\mathrm{ext}}$ is complex because increasing L means increasing the blockage effect to flow movement causing a weakening effect on $\Delta\psi_{\mathrm{ext}}$ and at the same time increasing L produces extra heating yielding an enhanced flow driving force which increases $\Delta\psi_{\mathrm{ext}}$. Furthermore, the blockage and heating effects of the fin is dependent on ε. The complex relation between L and $\Delta\psi_{\mathrm{ext}}$ is illustrated in Fig. 6 for ε values from 0° to 180° and $\kappa = 5$.

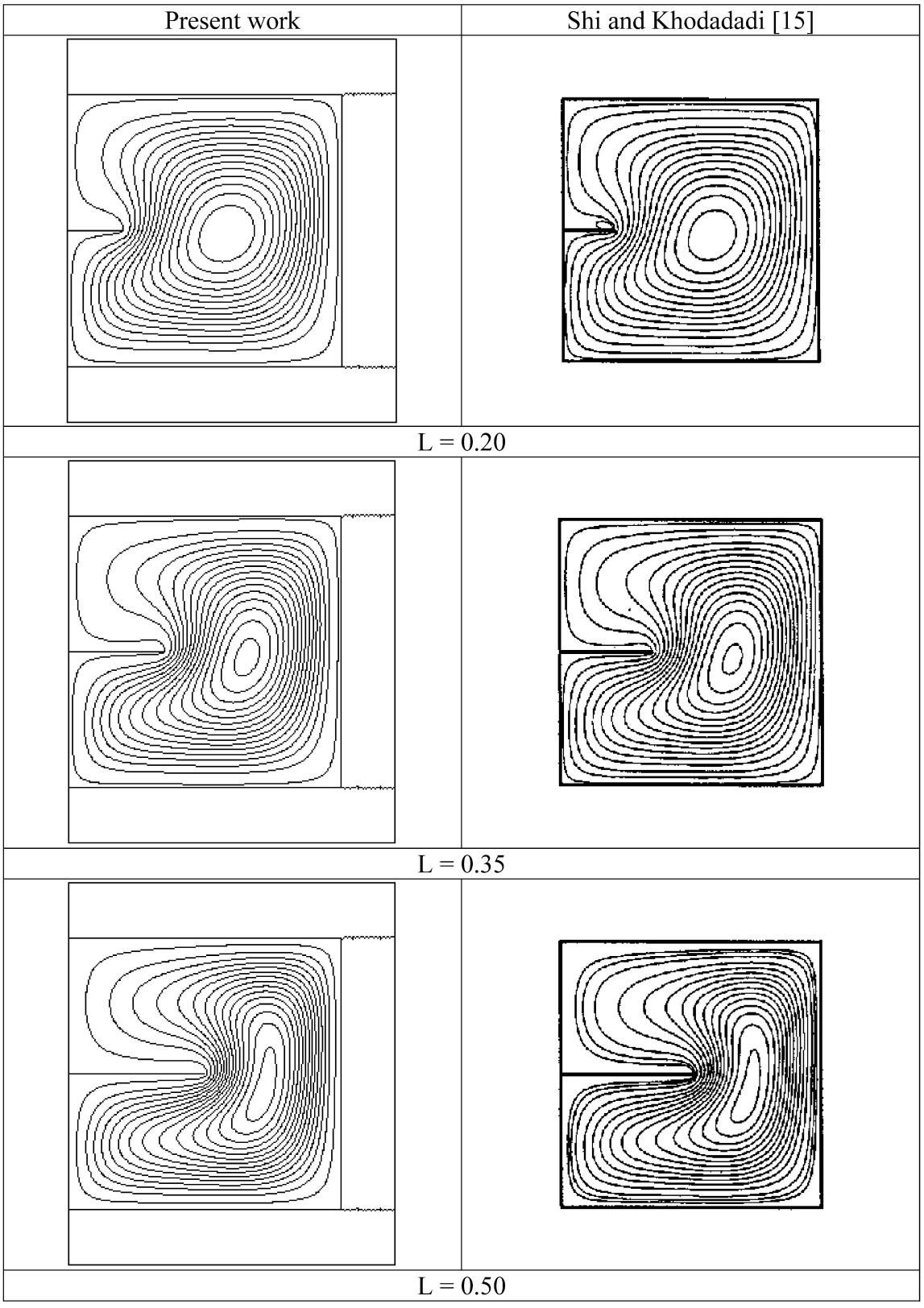

Fig. 2. Comparison of stream functions with those of Shi and Khodadadi [15] for $Ra = 10^4$.

The heat transfer behavior in the enclosure under consideration can be explored by the heat flux distributions on the solid–fluid interface. Fig. 7 presents the local Nusselt number Nu profiles at the heated surfaces (heated surface of the enclosure including both sides of the fin) for different values of ε and two values of κ ($\kappa = 1, \infty$) with $L = 0.2$, $Pr = 0.707$, $Ra = 10^5$. For clarity, the Nu profile for $\varepsilon = 90°$ is distinguished by a thicker line, the Nu profiles for $\varepsilon < 90°$ are designated

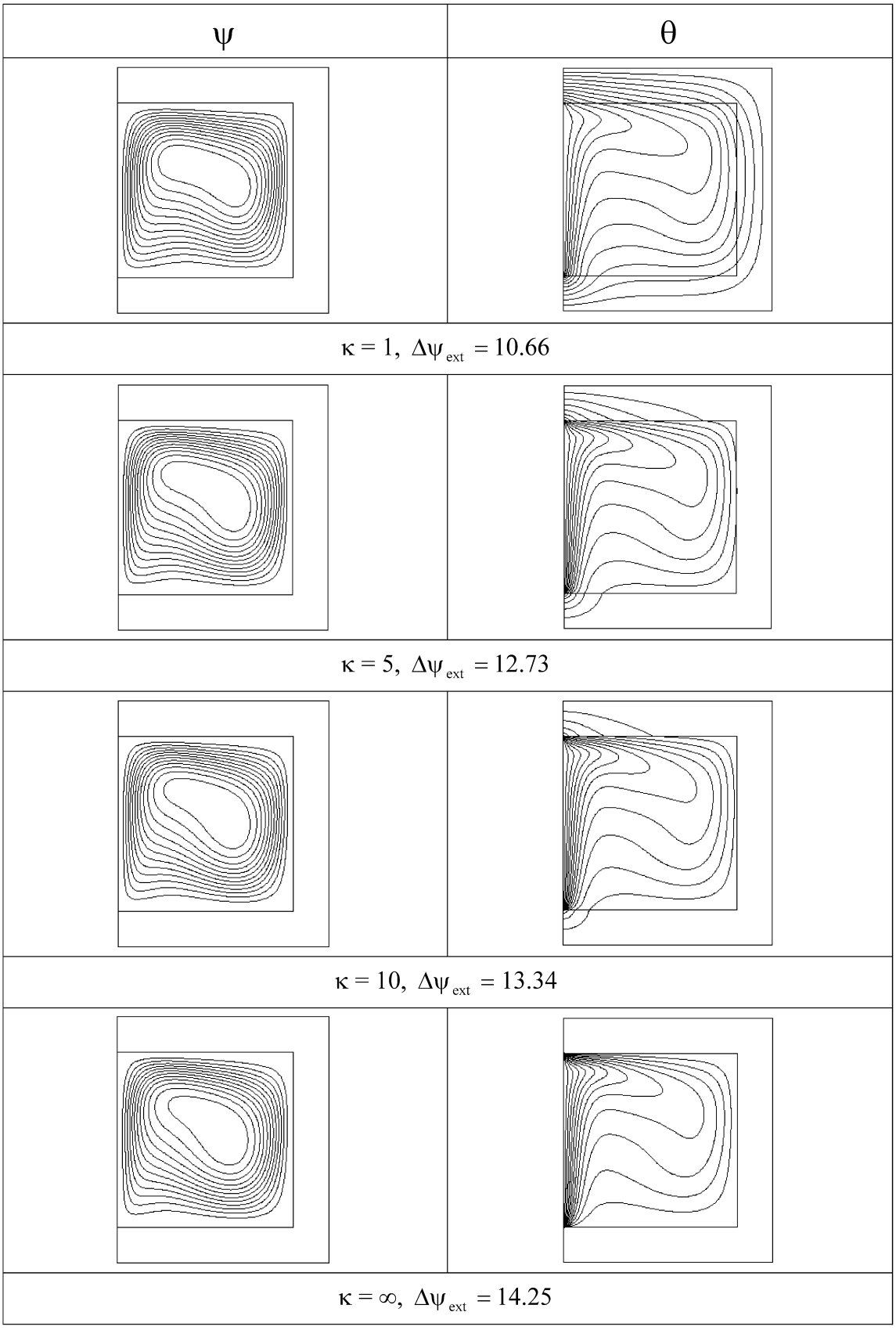

Fig. 3. Effects of κ on the contour maps of the streamlines and isotherms for enclosure without fin, $Pr = 0.707$, and $Ra = 10^5$.

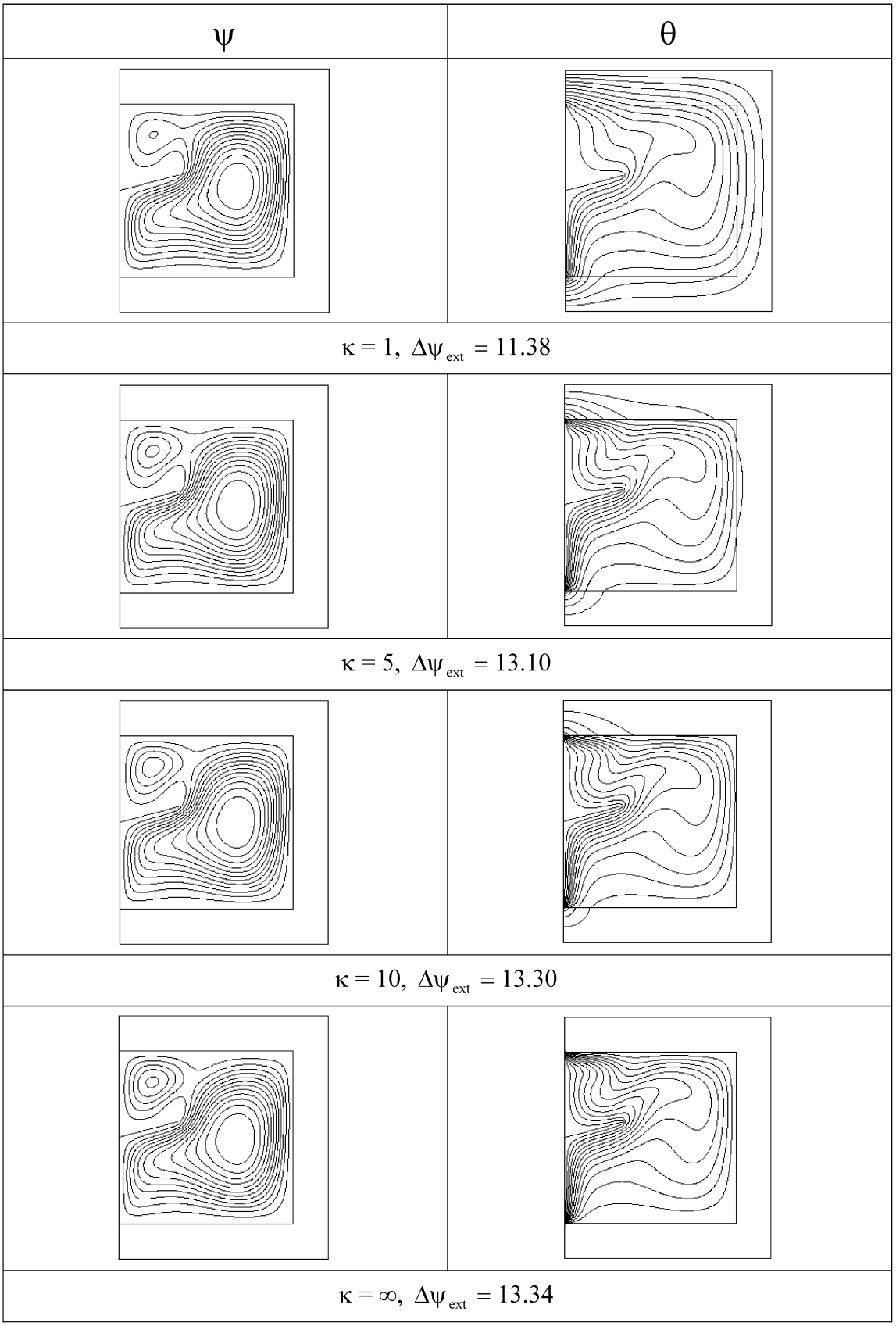

Fig. 4. Effects of κ on the contour maps of the streamlines and isotherms for enclosure with fin $\varepsilon = 105°$, $L = 0.35$, $Pr = 0.707$, and $Ra = 10^5$.

by solid thin lines, and the *Nu* profiles for $\varepsilon > 90^\circ$ are represented by dashed thin lines. In the absence of the thin fin, the local Nusselt number profile has two peaks near the intersections with the adjacent horizontal cold walls (i.e., $S = 0$ and $S = 1.0$). The sharp drop or increase in *Nu* near $S = 0$ and $S = 1$ respectively is a characteristics of boundary layer flow over a flat plate. The peak in the value of *Nu* in the neighborhood of $S = 1.0$ is always greater than that in the neighborhood of $S = 0$ due to flow direction which causes higher temperature gradient in the neighborhood of $S = 1.0$ compared to that in the

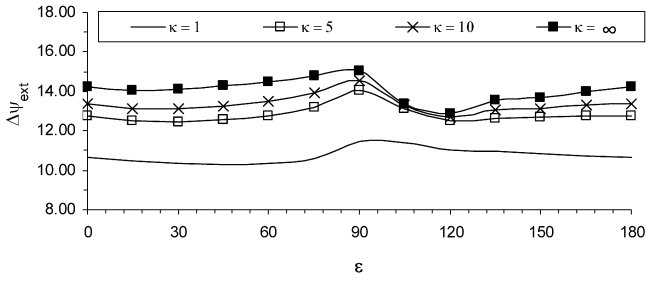

Fig. 5. Effects of κ and ε on $\Delta\psi_{\text{ext}}$ for $L = 0.35$, $Pr = 0.707$ and $Ra = 10^5$.

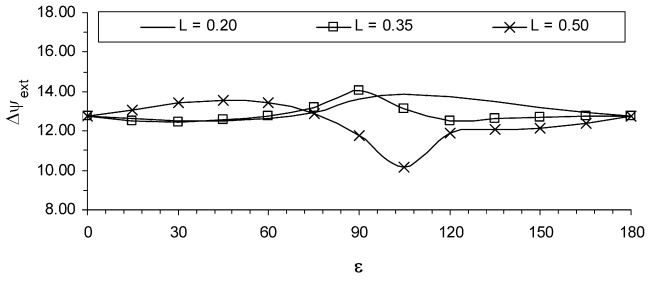

Fig. 6. Effects of L and ε on $\Delta\psi_{\text{ext}}$ for $\kappa = 5$, $Pr = 0.707$ and $Ra = 10^5$.

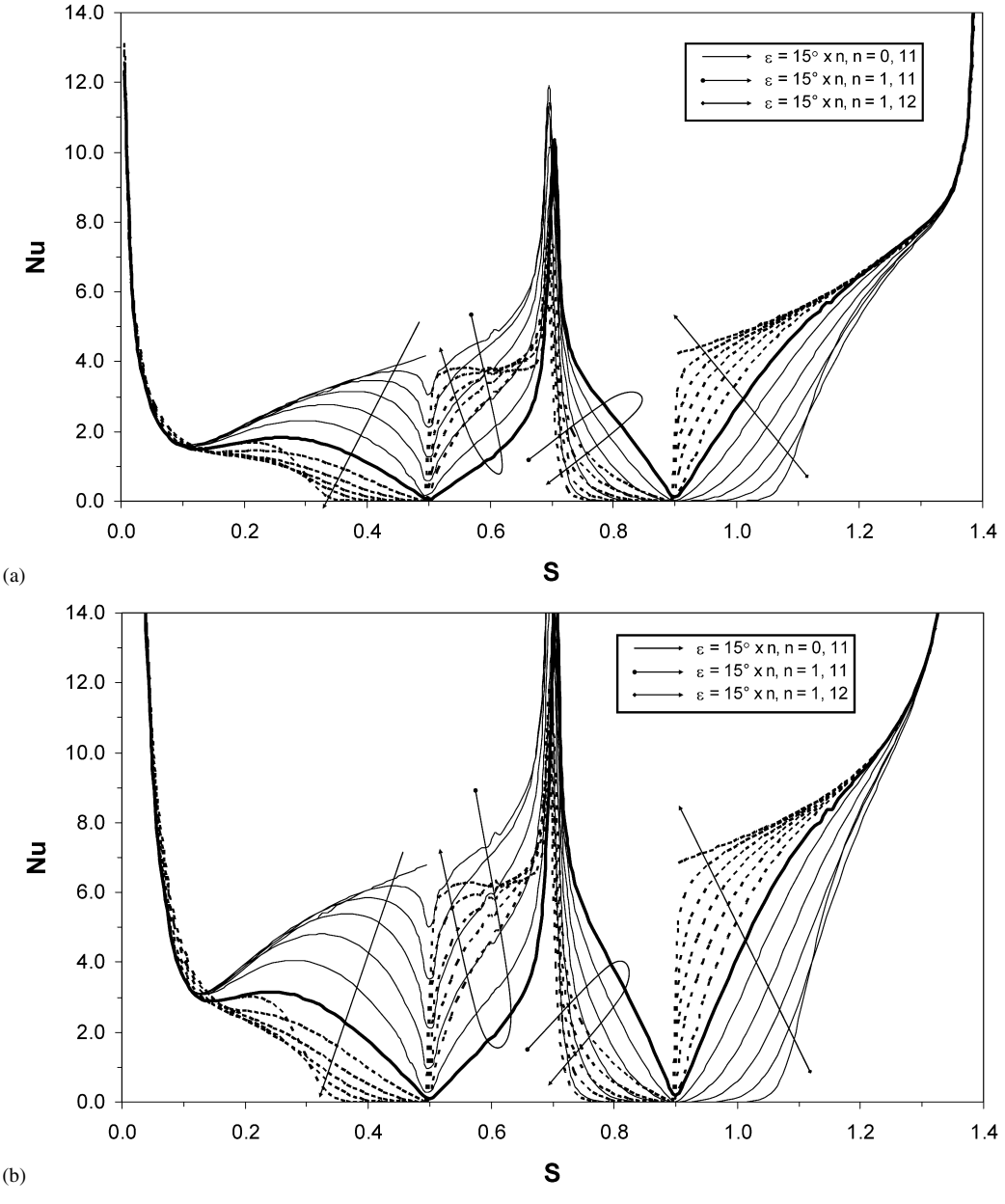

Fig. 7. Effects of ε on *Nu* for $L = 0.20$, $Pr = 0.707$, $Ra = 10^5$, and different values of κ: (a) $\kappa = 1$ and (b) $\kappa = \infty$.

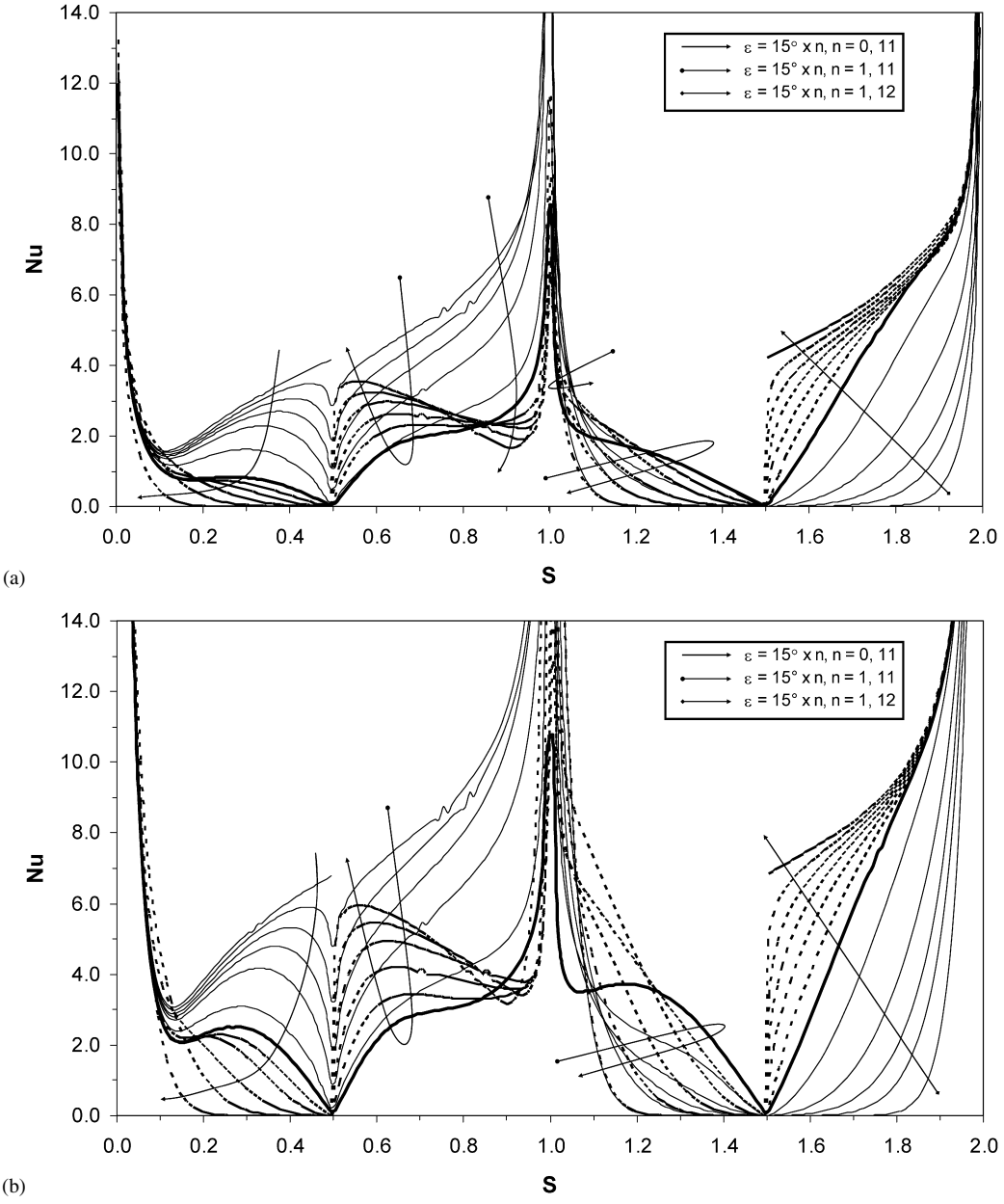

Fig. 8. Effects of ε on Nu for $L = 0.50$, $Pr = 0.707$, $Ra = 10^5$, and different values of κ: (a) $\kappa = 1$ and (b) $\kappa = \infty$.

neighborhood of $S = 0$. For the same reason, the Nu value for the no-fin case away from both ends (i.e., $S = 0$ and $S = 1.0$) increases as the dimensionless distance S increases. However, in the presence of a fin, the value of Nu exhibits a sharp reduction at the location of the wall/fin intersection where it becomes a minimum there due to flow stagnation. In principle, the attachment of a fin in the middle of the heated wall always reduces Nu for the heated wall by a ratio that is related to ε and L. An exception is at the upper end of the heated wall (i.e., S less than 0.135) where the value of Nu at high ε values increases till it reaches its peak within the range $135^\circ \leqslant \varepsilon \leqslant 150^\circ$ after which the value of Nu begins to decrease. This exception is due to the creation of a secondary recirculating cell in the area confined between the fin, heated wall, and upper cold wall.

In the presence of a thin fin, there are four heated surfaces in the considered enclosure: the upper and lower halves of the left wall, and the upper and lower surfaces of the fin. For the upper half of the heated wall, the value of Nu decreases as ε increases except for $\varepsilon = 165^\circ$ for which improvement in the value of Nu is observed at the upper segment near the top cold surface due to higher temperature differential caused by a local recirculating cell. However, Nu is directly related to ε for the lower half of the heated wall. This is mainly because of the inverse relation between ε and the blockage strength of the fin on the neighboring fluid flow. The relation between the local Nusselt number and ε is more complex for the upper and lower surfaces of the fin. For the upper surface of the fin, the value of Nu decreases as ε increases until the dip in the Nu profile is reached

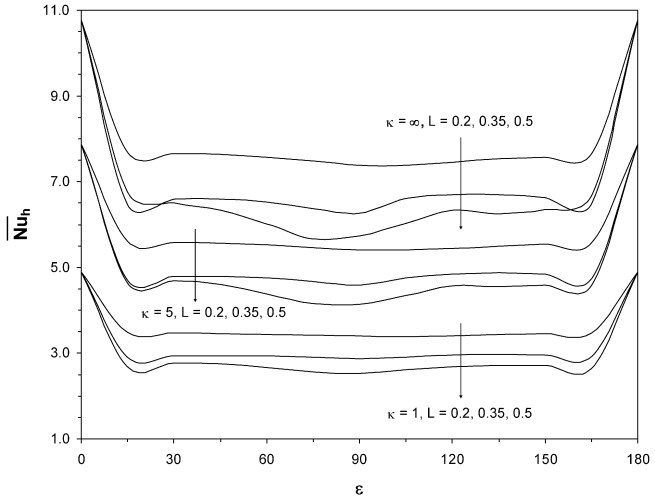

Fig. 9. Effects of ε, L, and κ on $\overline{Nu}_h$ for $Pr = 0.707$ and $Ra = 10^5$.

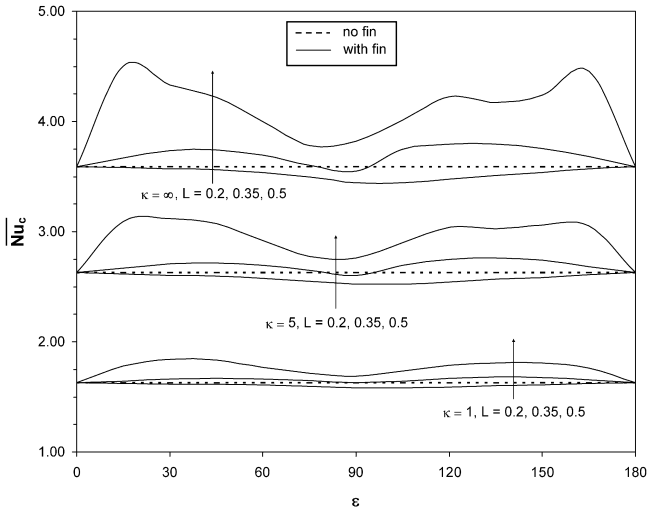

Fig. 10. Effects of ε, L, and κ on $\overline{Nu}_c$ for $Pr = 0.707$ and $Ra = 10^5$.

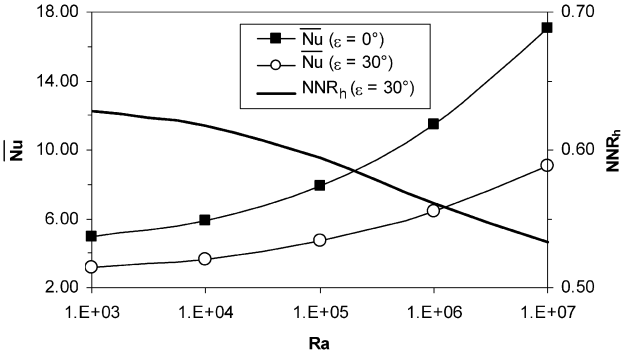

Fig. 11. Effects of Ra on $\overline{Nu}_h$ and NNR_h for $\varepsilon = 30°$, $L = 0.5$, $\kappa = 5$ and $Pr = 0.707$.

at $\varepsilon = 90°$ after which the value of Nu is directly related to ε within the area near the fin base, and inversely related with the area near the fin tip. Equivalently, for the lower surface of the fin, Nu increases as ε increases until the peak in the Nu profile is reached at $\varepsilon = 90°$ after which the value of Nu is inversely related to ε. Fig. 7 also shows that Nu is directly related to κ. It is predicted that the thick wall effect represented by small values of $\kappa(\kappa = 1)$ causes lower local Nusselt numbers compared to the case of thin wall ($\kappa = \infty$). A similar behavior of Nu profile was observed for $L = 0.35$, however, this is not shown due to space limitations. For this and next figure, it should be noted that in the absence of the thin fin, the Nu profile is split into two halves positioned at their corresponding locations for the finned cases. This is done for better illustration purposes.

Fig. 8 presents the Nu profiles at the heated surfaces for different ε values, $L = 0.5$, $Pr = 0.707$, $Ra = 10^5$, and two κ values: 1 and ∞. For $\kappa = 1$, the Nu profiles are related to ε in a manner similar to that observed for $L = 0.2$ and 0.35 except for the segments near the fin tip of the upper and lower fin surfaces. In the upper segment near the fin tip, the local Nusselt number is inversely related to ε. However, in the lower segment near the fin tip the local Nusselt number is inversely related to ε until the dip in the Nu profile is reached at $\varepsilon = 90°$ afterward Nu increases as ε increases. The Nu profiles for $\kappa = \infty$ behave in a similar manner to those corresponding to $\kappa = 1$ except at the upper and lower sectors near the fin tip. In both sectors near the fin tip, Nu is inversely related to ε until the Nu profile for $\varepsilon = 90°$ is reached then the Nu profiles do not follow a specific order.

Fig. 9 illustrates the influence of L and κ on the average Nusselt number at the heated surfaces $\overline{Nu}_h$ for ε values from 0° to 180°. It is clearly observed that ε, L, and κ have significant effects on $\overline{Nu}_h$. The figure demonstrates that $\overline{Nu}_h$ is directly related to κ, and inversely related with L. The exception to this rule is when $\kappa = \infty$ where $\overline{Nu}_h$ for $L = 0.5$ is higher than $\overline{Nu}_h$ for $L = 0.35$ at $\varepsilon \leqslant 25$ and $\varepsilon \geqslant 155$. It should be noted here that although the presence of fin always reduces $\overline{Nu}_h$, this does not mean that the heat flux from the heated surfaces to cold surface through the cavity is reduced. This fact is demonstrated in Fig. 10, which presents the effects of ε, L, and κ on $\overline{Nu}_c$. The dotted horizontal lines represent the no-fin cases for $\kappa = 1$, 5, and ∞. Clearly, the existence of a thin fin with $L = 0.2$ always reduces $\overline{Nu}_c$, while the existence of a thin fin with $L = 0.35$ or $L = 0.5$ always increases $\overline{Nu}_c$ except for $L = 0.35$, $\kappa = 5$ or ∞, and in the vicinity of $\varepsilon = 90°$ $\overline{Nu}_c$ is decreased.

Finally, Fig. 11 depicts the influence of the Rayleigh number Ra on the average Nusselt number of the heated surfaces $\overline{Nu}_h$ for $\varepsilon = 0°$, 30°and the heated surfaces Nusselt number ratio NNR_h for $\varepsilon = 30°$. Clearly, $\overline{Nu}_h$ is directly proportional to Ra, while NNR_h is inversely related to Ra in the range $10^3 \leqslant Ra \leqslant 10^7$. That is, $\overline{Nu}_h$ increases while NNR_h decreases as Ra increases.

5. Conclusions

Conjugate natural convection heat transfer in a square enclosure which has three thick cooled thick walls and one thin heated vertical wall with a heated inclined thin fin attached to its middle was studied numerically. The governing equations for this investigation were put in the dimensionless vorticity-stream function formulation and were solved by the finite volume technique. Graphical results for the streamline and temperature contours for several parametric conditions were presented and discussed. It was found that the thin fin inclination angle and

length, and solid-to-fluid thermal conductivity ratio have significant effects on the local and average Nusselt number at the heated surfaces of the enclosure/fin system. In general, the presence of an inclined thin fin reduces the average Nusselt number at the heated surfaces in an unordered way. This is because the addition of a fin to an enclosure has two counter-acting effects: restraining natural convection and increasing heating surface. Therefore, in design applications, it is possible to control heat transfer through an enclosure by proper selection of both fin inclination angle and length based on the associated Rayleigh number, the walls thickness and thermal conductivity ratio. With respect to heat transfer optimization, which requires average Nusselt number analyses over the whole fin inclination angle range, it was concluded that the worst heat transfer performance was close to $\varepsilon = 90^\circ$ for $Pr = 0.707$ and the ranges for L, κ and Ra considered in the current study.

References

[1] K.E. Starner, H.N. McManus, An experimental investigation of free convection heat transfer from rectangular fin-arrays, J. Heat Transfer (1963) 273–278.

[2] J.R. Welling, C.B. Wooldridge, Free convection heat transfer coefficient from rectangular vertical fins, J. Heat Transfer (1965) 439–444.

[3] F. Harahap, H.N. McManus, Natural convection heat transfer from horizontal rectangular fin arrays, J. Heat Transfer (1967) 32–38.

[4] P. Oosthuizen, J.T. Paul, Free convection heat transfer in a cavity fitted with a horizontal plate on the cold wall, in: S.M. Shenkman, et al. (Eds.), Advances in Enhanced Heat Transfer, in: ASME-HTD, vol. 43, 1985, pp. 101–107.

[5] S. Shakerin, M. Bohn, R.I. Loehrke, Natural convection in an enclosure with discrete roughness elements on a vertical heated wall, Int. J. Heat Mass Transfer 31 (1988) 1423–1430.

[6] R.L. Frederick, Natural convection in an inclined square enclosure with a partition attached to its cold wall, Int. J. Heat Mass Transfer 32 (1989) 87–94.

[7] R.L. Frederick, A. Valencia, Heat transfer in a square cavity with a conducting partition on its hot wall, Int. Commun. Heat Mass Transfer 16 (1989) 347–354.

[8] A. Nag, A. Sarkar, V.M.K. Sastri, Natural convection in a differentially heated square cavity with a horizontal partition plate on the hot wall, Comput. Methods Appl. Mech. Engrg. 110 (1993) 143–156.

[9] M. Hasnaoui, P. Vasseur, E. Bilgen, Natural convection in rectangular enclosures with adiabatic fins attached on the heated wall, Warme and Stoffubertragung 27 (1992) 357–368.

[10] R. Scozia, R.L. Frederick, Natural convection in slender cavities with multiple fins attached on an active wall, Numer. Heat Transfer, Part A 20 (1991) 127–158.

[11] G.N. Facas, Natural convection in a cavity with fins attached to both vertical walls, J. Thermophys. Heat Transfer 7 (1993) 555–560.

[12] E.K. Lakhal, M. Hasnaoui, E. Bilgen, P. Vasseur, Natural convection in inclined rectangular enclosures with perfectly conducting fins attached on the heated wall, Heat Mass Transfer 32 (1997) 365–373.

[13] E. Bilgen, Natural convection in enclosures with partial partitions, Renewable Energy 26 (2002) 257–270.

[14] X. Shi, J.M. Khodadadi, Laminar fluid flow and heat transfer in a lid-driven cavity due to a thin fin, ASME J. Heat Transfer 124 (6) (2002) 1056–1063.

[15] X. Shi, J.M. Khodadadi, Laminar natural convection heat transfer in a differentially heated square cavity due to a thin fin on the hot wall, ASME J. Heat Transfer 125 (4) (2003) 624–634.

[16] E. Bilgen, Natural convection in cavities with a thin fin on the hot wall, Int. J. Heat Mass Transfer 48 (2005) 3493–3505.

[17] A. Ben-Nakhi, A. Chamkha, Effect of length and inclination of a thin fin on natural convection in a square enclosure, Numer. Heat Transfer Part A: Appl. 50 (4) (2006) 389–407.

[18] D.M. Kim, R. Viskanta, Heat transfer by conduction, natural convection and radiation across a rectangular cellular structure, Int. J. Heat Fluid Flow 5 (4) (1984) 205–213.

[19] D.A. Kaminski, C. Prakash, Conjugate natural convection in a square enclosure: Effect of conduction in one of the vertical walls, Int. J. Heat Mass Transfer 29 (12) (1986) 1979–1988.

[20] Z.G. Du, E. Bilgen, Coupling of wall conduction with natural convection in a rectangular enclosure, Int. J. Heat Mass Transfer 35 (8) (1992) 1969–1975.

[21] A. Liaqat, A.C. Baytas, Conjugate natural convection in a square enclosure containing volumetric sources, Int. J. Heat Mass Transfer 44 (2001) 3273–3280.

[22] S.V. Patankar, Numerical Heat Transfer and Fluid Flow, Hemisphere, Washington, DC, 1980.